Harmonic Analysis of Tides at Bonga Oil Field, Nigeria

O.T. Badejo[1], P. Evarie[2], N. Anorue[1] and S. Alademomi[1]
[1]Department of Surveying and Geoinformatics, University of Lagos
[2]Geomatics Department, Shell Nigeria Exploration and Production Company
E-mail: shegunbadejo@yahoo.com

Abstract
Oil exploration and exploitation activities are being moved from swamp and shallow waters to deep offshore locations in Nigeria, and therefore, there is a need to provide predicted tides to support oil and gas operations in deep offshore environment. In this work, 51 days' water level observations derived from water pressure data recorded by AANDERAA Water Level Recorder WLR 7 at a depth of 1,000 m at Bonga field were analysed and used to carry out tidal harmonic analysis. Eleven tidal constituents were used for the harmonic analysis. Astronomical arguments (v + u) and the nodal factor (f) were computed for each tidal constituent with a programme written in Matlab environment. The amplitudes and the phase lags for each constituent were calculated and tidal predictions beginning from the initial time of tidal observation in September 11, 2010 to January 2019 were done at 10 minutes' intervals. Statistical analysis of predicted tides and observed tidal data was done. The highest deviation of the predicted tides from the observed tidal data is 0.0008 m, while the Root Mean Square Error is 0.0003 m. Autocorrelation at lags 1 to 30 for the residuals of observed and predicted tidal data shows that there is no significant correlation in the series of the 30 lags. The series of residuals of observed and predicted data is white noise. The accuracy of this work is high enough for offshore operations in Bonga Field.

Keywords: Bonga Field, Harmonic Analysis, Tidal Observations, Predictions

1.0 INTRODUCTION

Tides are periodic rises and falls in water level. They usually arise as a result of gravitational attraction of the moon and sun on the earth. Water level recordings are done out with the aid of tide gauges nearshore in Nigeria. Now that oil exploration and exploitation activities are being moved from swamp and shallow waters to deep offshore locations in Nigeria, there is a need to use modern and appropriate tide measuring equipment offshore and also investigate the nature and effect of tides in deep offshore environment.

The Bonga oilfield in Nigeria is located in Oil Mining Lease (OML) 118. This lease extends over an area of 1167 km^2. Bonga oilfield is at a water depth of 1,000 m. The oilfield was discovered in 1996. Federal Government of Nigeria approved the development of Bonga oilfield in 2002. Oil production began in Bonga oilfield in November 2005. Bonga oilfield produces crude oil and natural gas with the aid of a floating production, storage and off-take (FPSO) vessel. Crude oil is offloaded to oil tankers through a single point mooring (SPM) buoy while the gas from Bonga oilfield is exported through a range of pipelines to Bonny NLNG plant. Bonga oilfield is operated by Shell Nigeria Exploration and Production Company (SNEPCo) and owned by Shell Nigeria (55 %), Exxon (20 %), Nigerian AGIP (12.5 %) and Elf Petroleum (12.5 %).

2.0 METHODOLOGY

This work is aimed at using tidal predictions to assist and support deep water oil exploration and exploitation activities in Bonga oilfield, offshore Nigeria. The methodology adopted for this study includes water level recordings using Water Level Recorder WLR 7, extraction of tidal data from recordings from the water level recorder. Extracted tidal data from the Water Level Recorder were subjected to tidal harmonic analysis and prediction.

2.1 Data Acquisition

Water Level Recorder WLR 7 was used for acquiring tidal data in Bonga oilfield. The Water Level Recorder WLR7 is a high precision recording equipment useful for recording water level nearshore and offshore. The water level is calculated by measuring the hydrostatic pressure with an ultra-precise quartz pressure sensor. Once the water density and atmospheric pressure are known, the water level can then be determined. The operational depth of the Water Level Recorder can be limited by the range of the pressure transducer. The mechanical parts of Water Level Recorder WLR 7 are strengthened to withstand a pressure down to 6000 m water depth.

Water level data were recorded by Water Level Recorder WLR 7 by Geomatics Department of the SNEPCo for 51 days. The water level recordings were done at ten minutes intervals from September 11, 2010 to November 1, 2010. A total of 8987 datasets were recorded during this period. The 10 minute interval recorded data were reduced to 1224 hourly data. The 1224 hourly readings were then converted to depth data using Eq. 1.

$$D = \frac{0.001(P_{wd} - P_{atmos})}{dg} \quad (1)$$

where, D is the depth of water, P_{wd} is the water pressure at the depth of the Water Level Recorder WLR 7 (Pa), P_{atmos} is the atmospheric Pressure of Bonga oilfield (101000 Pa), d is the water density of Bonga oilfield (1.03017 Kgm^{-3}), and g is the force of gravity (9.78334 ms^{-2}).

The least water depth recorded was set as the chart datum, while water levels above this chart datum were taken as tidal data.

Prior to the commencement of tidal harmonic analysis of the tidal data, the observed tidal data were made to go through a median filter to remove spikes in the data. The essence of the median filter is to run through the tidal data one by one, substituting each tidal data with the median of neighboring tidal data).

2.2 Harmonic Analysis of Tides

The fundamental equation for harmonic analysis of tide is given by Doodson and Warburg (1941) as Eq. 2:

$$h(t) = S_0 + \sum_{t=1}^{n} (H_i Cos[\omega_i t + \alpha_i]) \quad (2)$$

where; ω_i is the angular frequency of the tidal constituent I, H_i is the amplitude of tidal constituent I, S_o is the height of average water level above the datum used, t is time, n is the number of harmonic constituents, α_i is the phase of each harmonic constituent.

Due to the slow rotation of the orbit of the moon with a period of about 18.61 years, the magnitude, H, and phase, α, of each harmonic constituent changes slowly on either side of the values they would have if the moon's orbit were constant. To account for these changes, a nodal factor f and astronomical argument (v + u) are usually brought in to modify Eq. 2 (Eluwa, 1991). Introducing the nodal factor f and (v+u) gives Eq. 3.

$$h(t) = S_0 + \sum_{t=1}^{n} (f_i H_i Cos[\omega_i t + (v_i + u_i - \alpha_i)\,]) \quad (3)$$

where, v is the phase angle at time zero, u is the nodal angle, and f is the nodal factor.

Eleven tidal constituents were used for the harmonic analysis; the eleven tidal constituents are shown in **Table 1**.

Table 1: Tidal Constituents used for Harmonic Analysis

S/N	Constituent Name	Constituent Frequency (ω_i)
1.	M2	28.9841042
2.	S2	30.0000000
3.	N2	28.4397295
4.	K2	30.0821373
5.	K1	15.0410686
6.	O1	13.9430356
7.	P1	14.9589314
8.	MSf	1.0158958
9.	2N2	27.8953548
10.	M4	57.9682084
11.	MS4	58.9841042

Mathematical equations for calculating v and u are given in **Tables 2 and 3** according to Schureman (1958) with some minor changes due to the direct use of the original astronomical parameters (Stravisi, 1983).

Table 2 summarizes the fundamental astronomical parameters. The time dependent auxiliary coefficients (c) are introduced for their recurrent use. Their numerical values at the beginning of 1985 are given, together with the annual variations taken between 1980 and 1990; final values can be rounded to six decimal digits. The longitudes of lunar and solar elements (d) define the long period time dependence of the constituent arguments v; they are expressed as a function of T as in Eq. 4.

$$T = \frac{\left(365n + int\left[\frac{n-1}{4}\right] + 0.5\right)}{36525} \tag{4}$$

where, T is time expressed in Julian centuries (36 525 d), reckoned from Greenwich mean noon, December 31, 1899 (Gregorian calendar); m is time after 0 h, January 1, 1900 in years and the integer part of (n - 1)/4 accounts for the leap years (Schureman, 1958; Stravisi, 1983). The time dependent elements of the moon's orbit (e) define, according to Schureman (1958), f (nodal factor) and u (nodal angle).

Astronomical arguments (v+u) and corresponding nodal factor (f) were calculated for seven constituents for each observation period in Matlab programming environment using equations in **Tables 2 and 3**.

The Nodal factors f and astronomical arguments v and u for the remaining four tidal constituents were derived from the nodal factors and astronomical arguments v and u of the seven constituents given in **Table 3**. **Table 4** shows the relationships between the various nodal factors and astronomical arguments.

Table 2: Astronomical Parameters of Use in Tidal Computations

a) Constants			
c	$= 3.844\,03 \times 10^8$ m	mean earth-moon distance	
c_1	$= 1.495\,042\,01 \times 10^{11}$ m	mean earth-sun distance	
S/E	$= 332\,488 \pm 43$	sun/earth mass ratio	
M/E	$= 12\,289 \pm 4 \times 10^{-6} = 1/81.37$	moon/earth mass ratio	
S/M	$= 2.705\,455 \times 10^7$	sun/moon mass ratio	
S'	$= (c/c_1)^3$ S/M $= 0.459\,875\,64$	solar factor	
e	$= 0.054\,900\,56$	eccentricity of moon's orbit	
i	$= 5.145\,376\,28°$	inclination of moon's orbit to plane of ecliptic	
b) Time dependent parameters			
n		time after 1900, in years	
e_1	$= 0.016\,751\,04 - 4.180 \times 10^{-7}\,n - 1.26 \times 10^{-11}\,n^2$	eccentricity of earth's orbit	
ω	$= 23.452\,294° - 1.301\,11° \times 10^{-4}\,n$	obliquity of the ecliptic	
c) Time dependent auxiliary coefficients		**Numerical value, 1985**	**Increment, per year**
A	$= S'(1 + 3/2\,e_1^2)/(1 + 3/2\,e^2)$		
A_1	$= \cos i \cos \omega$	0.913 771 493	+ 0.000 000 900
A_2	$= \sin i \sin \omega$	0.035 676 679	− 0.000 000 187
A_3	$= \cos \frac{1}{2}(\omega - i) / \cos \frac{1}{2}(\omega + i)$	1.018 819 128	− 0.000 000 108
A_4	$= \sin \frac{1}{2}(\omega - i) / \sin \frac{1}{2}(\omega + i)$	0.643 957 699	− 0.000 001 671
A_5	$= A \sin 2\omega$	0.334 316 893	− 0.000 001 429
A_6	$= A \sin^2 \omega$	0.072 478 792	− 0.000 000 761
B_1	$= \{\cos \frac{\omega}{2} \cos \frac{i}{2}\}^{-4}$	1.092 333 626	− 0.000 001 029
B_2	$= \{A_5 + (1 - 3/2 \sin^2 i) \sin 2\omega\}^{-2}$	0.897 663 509	+ 0.000 007 647
B_3	$= \{A_6 + (1 - 3/2 \sin^2 i) \sin^2 \omega\}^{-2}$	19.098 898 614	+ 0.000 400 363
B_4	$= \{\sin \omega \cos^2 \frac{\omega}{2} \cos^4 \frac{i}{2}\}^{-1}$	2.632 568 903	+ 0.000 012 547
B_5	$= 2 A_5 B_2$	0.600 208 150	+ 0.000 002 548
B_6	$= 2 A_6 B_3$	2.768 530 194	+ 0.000 028 978
B_7	$= \{1 + (1 - 3/2 \sin^2 i)/A\}^{-2} = B_2 A_5^2 = B_3 A_6^2$	0.100 329 862	− 0.000 000 003
d) Longitude of lunar and solar elements (3)			
T	time in Julian centuries (36 525 d), reckoned from Greenwich mean noon, December 31, 1899		
h	$= 279.696\,678° + 36\,000.768\,925°\,T + 3.025° \times 10^{-4}\,T^2$	mean longitude of sun	
s	$= 270.437\,422° + 481\,267.892\,000°\,T + 2.525° \times 10^{-3}\,T^2 + 1.89° \times 10^{-6}\,T^3$	mean longitude of moon	
p	$= 334.328\,019° + 4\,069.032\,206°\,T - 1.034\,4° \times 10^{-2}\,T^2 - 1.25° \times 10^{-5}\,T^3$	longitude of lunar perigee	
N	$= 259.182\,533° - 1\,934.142\,397°\,T + 2.106° \times 10^{-3}\,T^2 + 2.22° \times 10^{-6}\,T^3$	longitude of moon's node	
e) Time dependent elements of the lunar orbit (3)			
I	$= \arccos\{A_1 - A_2 \cos N\}$	obliquity of lunar orbit with respect to earth's equator	
C	$= \arctan\{A_3 \tan N/2\}$		
ν	$= C - \arctan\{A_4 \tan N/2\}$	right ascension of lunar intersection	
ν'	$= \arctan\{(\sin 2I \sin \nu)/(A_5 + \sin 2I \cos \nu)\}$	auxiliary term for K_1	
$2\nu''$	$= \arctan\{(\sin^2 I \sin 2\nu)/(A_6 + \sin^2 I \cos 2\nu)\}$	auxiliary term for K_2	
ξ	$= N + \nu - 2C$	longitude in moon's orbit of lunar intersection	

(1) American Ephemeris and Nautical Almanac
(2) Smithsonian Physical Tables
(3) Schureman (1958)

Source: (Stravisi, 1983)

Table 3: Time Dependent Nodal Factors, Arguments and Speeds of Seven Major Harmonic Component Tides

	f	V (t) (1)	u	σ (2)
M_2	$B_1 \cos^4 \frac{I}{2}$	$2\tau - 2s + 2h$	$2\xi - 2\nu$	$28.984\,104\,214 - 10.14 \times 10^{-9}\,T = 28.984\,104\,205$
S_2	1	2τ 0	0	30
N_2	$B_1 \cos^4 \frac{I}{2}$	$2\tau - 3s + 2h + p$	$2\xi - 2\nu$	$28.439\,729\,516 - 28.16 \times 10^{-9}\,T = 28.439\,729\,492$
K_2	$\{B_3 \sin^4 I + B_6 \sin^2 I \cos 2\nu + B_7\}^{1/2}$	$2\tau + 2h$	$-2\nu''$	$30.082\,137\,278 + 1.38 \times 10^{-9}\,T = 30.082\,137\,279$
K_1	$\{B_2 \sin^2 2I + B_5 \sin 2I \cos \nu + B_7\}^{1/2}$	$\tau + h - 90°$	$-\nu'$	$15.041\,068\,639 + 0.69 \times 10^{-9}\,T = 15.041\,068\,640$
O_1	$B_4 \sin I \cos^2 \frac{I}{2}$	$\tau - 2s + h + 90°$	$2\xi - \nu$	$13.943\,035\,575 - 10.84 \times 10^{-9}\,T = 13.943\,035\,566$
P_1	1	$\tau - h + 90°$	0	$14.958\,931\,361 - 0.69 \times 10^{-9}\,T = 14.958\,931\,360$

(1) $\tau = 15°\,t + 180°$ is the hour angle of the mean sun; t is Greenwich time in hours.
(2) Angular speed in °/h; terms in T^2, computed for T = 1, are enclosed.
Constant speeds refer to T = 0.85, year 1985.

Source: (Stravisi, 1983)

The Nodal factors f and astronomical arguments v and u for the remaining four tidal constituents were derived from the nodal factors and astronomical arguments v and u of the seven constituents given in **Table 3**. **Table 4** shows the relationships between the various nodal factors and astronomical arguments.

Table 4: Relationships between Various Nodal Factors and Astronomical Arguments

S/N	Constituent Name	Constituent Speed (ω_i)	Nodal Factor (f_i)	Astronomical Argument (V_i+U_i)
1.	MSf	1.0158958	f of M_2	360-(v+u) of M_2
2.	$2N_2$	27.8953548	f of M_2	2x(v+u) of N_2- (v+u) of M_2
3.	M_4	57.9682084	(f of M_2) Squared	2x(v+u) of M_2
4.	MS_4	58.9841042	f of M_2	(v+u) of M_2

The tidal harmonic analysis model in Eq. 3 can be expanded using trigonometric functions as in Eq. 5:

$$h(t) = S_0 + \sum_{t=1}^{n}(f_i H_i Cos[\omega_i t + (v_i + u_i)]\, Cos\, \alpha_i) + \sum_{t=1}^{n}(f_i H_i Sin[\omega_i t + (v_i + u_i)]\, Sin\, \alpha_i) \quad (5)$$

Let $A_i = H_i Cos\, \alpha_i$ and $B_i = H_i Sin\, \alpha_i$

The tidal harmonic and prediction model can be expressed in Eq. 6.

$$h(t) = S_0 + \sum_{t=1}^{n}((A_i f_i Cos[\omega_i t + (v_i + u_i)]) + (B_i f_i Sin[\omega_i t + (v_i + u_i)])) \quad (6)$$

A Matrix will therefore be created in the form of Eq. 7:

$$A = \begin{bmatrix} S_0 & A_1 & B_1 & A_2 & B_2 \\ 1 & f_1 cos[w_1 t_1 + \{v_1 + u_1\}] & f_1 sin[w_1 t_1 + \{v_1 + u_1\}] & f_2 cos[w_2 t_1 + \{v_1 + u_1\}] & f_2 cos[w_2 t_1 + \{v_1 + u_1\}] \ldots \\ 1 & f_1 cos[w_1 t_2 + \{v_1 + u_1\}] & f_1 cos[w_1 t_2 + \{v_1 + u_1\}] & f_2 cos[w_2 t_2 + \{v_1 + u_1\}] & f_2 cos[w_2 t_2 + \{v_1 + u_1\}] \ldots \\ 1 & f_1 Cos\, [\omega_1 t_n + \{v_1 + u_1\}] & f_1 Sin\, [\omega_1 t_n + \{v_1 + u_1\}] & f_2 Cos\, [\omega_2 t_n + \{v_1 + u_1\}] & f_2 Sin\, [\omega_2 t_n + \{v_1 + u_1\}] \ldots \end{bmatrix} \quad (7)$$

A total of twenty-three unknowns would be solved for in the trigonometric equation. A total of 1224 observed tidal data (51 days data) form the vector of observations. Least squares adjustment method was used to solve for the unknown parameters. The least squares adjustment solution is given as in Eqs. 8 – 10:

$$X = (A^T PA)^{-1} A^T PL \quad (8)$$

$$X = [S_0, A_1, B_1, \ldots \ldots \ldots A_n, B_n]^T \quad (9)$$

$$L = [h_1, h_2, \ldots \ldots \ldots h_n]^T \quad (10)$$

The normal equation $(A^T PA)$ is near singular and thus the unknown parameters X were determined by using conjugate gradient method. This method was discussed extensively in Badejo *et al*. (2012). With the values of the unknown parameters in Eq. 9 computed, and the values of f_i and (v_i + u_i) obtained from **Tables 2 and 3**, (Badejo, Evarie and Anorue, 2013) solve for the harmonic constant α_i as expressed in Eqs. 11a and b:

$$Tan\alpha_i = \frac{B_i}{A_i} = \frac{H_i\, Sin\alpha_i}{H_i\, Cos\alpha_i} \quad (11a)$$

$$\alpha_i = Tan^{-1}\left(\frac{B_i}{A_i}\right) \quad (11b)$$

H_i can also be determined from the following relationship in Eqs. 12a and b:

$$B_i = H_i Sin\alpha_i \quad (12a)$$

$$H_i = \frac{B_i}{Sin\ \alpha_i} \tag{12b}$$

3.0 RESULTS AND DISCUSSION

The results and analysis of results of this work are presented in sections 3.1 and 3.2.

The results of the least squares harmonic analysis are presented in this section. **Table 5** shows the solution of the least squares adjustment and the residuals from the least squares adjustment. The tidal characteristics of the eleven tidal constituents used for the adjustment are shown in **Table 6**; while **Table 7** shows tidal prediction for part of January 1, 2017.

Table 5: Least Squares Solution and Residuals from Least Squares Adjustment

S/N	Least Squares Solution (X)	Residuals from Adjustment (V=AX-L)
1	1.0048	6.94E-18
2	-0.3494	-1.18E-16
3	0.3673	-1.09E-16
4	0.1085	9.76E-19
5	-0.1335	4.34E-19
6	0.0731	4.88E-19
7	0.0971	-6.67E-18
8	-0.0336	1.08E-18
9	-0.0078	-1.12E-17
10	0.1220	4.34E-19
11	0.0390	3.79E-19
12	-0.0197	-2.03E-18
13	-0.0192	-1.95E-18
14	0.0245	1.08E-19
15	0.0265	-4.07E-20
16	-0.0116	-5.42E-19
17	0.0231	-5.42E-19
18	0.0132	-1.28E-16
19	-0.0314	-9.63E-17
20	0.0128	-7.45E-17
21	0.0060	7.13E-17
22	-0.0044	1.67E-17
23	-0.0080	1.24E-16

Table 6: Tidal Characteristics of the Eleven Constituents used for Least Squares Adjustment

S/N	Constituent Name	Constituent Frequency (ω_i)	Amplitudes (H) (m)	Nodal Factor (F)	V+U (Deg)	Phase Lag (Deg)
1	M2	28.9841042	0.5070	0.9865	134.0246	133.5738
2	S2	30.0000000	0.1721	1.0000	360.0000	309.0952
3	N2	28.4397295	0.1215	0.9865	13.8260	53.0122
4	K2	30.0821373	0.0345	1.1252	232.8068	192.9887
5	K1	15.0410686	0.1281	1.0543	202.1960	17.7104
6	O1	13.9430356	0.0275	1.0873	182.1322	224.3631
7	P1	14.9589314	0.0361	1.0000	70.5148	47.2327
8	MSf	1.0158958	0.0258	0.9865	225.9754	116.6327
9	2N2	27.8953548	0.0341	0.9865	296.4901	292.8258
10	M4	57.9682084	0.0141	0.9732	268.0493	25.2767
11	MS4	58.9841042	0.0092	0.9865	134.0246	241.3641

Table7: Tidal Predictions for Part of January 1 2017

S/N	Year	Month	Day	Hour	Min	Predicted Tide Above Chart Datum (m)
1	2017	1	1	0	0	0.6150
2	2017	1	1	0	10	0.6365
3	2017	1	1	0	20	0.6617
4	2017	1	1	0	30	0.6901
5	2017	1	1	0	40	0.7216
6	2017	1	1	0	50	0.7558
7	2017	1	1	1	0	0.7924
8	2017	1	1	1	10	0.8309
9	2017	1	1	1	20	0.8711
10	2017	1	1	1	30	0.9127
11	2017	1	1	1	40	0.9551
12	2017	1	1	1	50	0.9981
13	2017	1	1	2	0	1.0414
14	2017	1	1	2	10	1.0846
15	2017	1	1	2	20	1.1273
16	2017	1	1	2	30	1.1693
17	2017	1	1	2	40	1.2104
18	2017	1	1	2	50	1.2501
19	2017	1	1	3	0	1.2883
20	2017	1	1	3	10	1.3247
21	2017	1	1	3	20	1.3592
22	2017	1	1	3	30	1.3914
23	2017	1	1	3	40	1.4213
24	2017	1	1	3	50	1.4486
25	2017	1	1	4	0	1.4732
26	2017	1	1	4	10	1.4949
27	2017	1	1	4	20	1.5137
28	2017	1	1	4	30	1.5294
29	2017	1	1	4	40	1.5418
30	2017	1	1	4	50	1.5509

The result of the sample observed in September 11, 2010 to January 2019 and the predicted tidal data above chart datum are presented in **Table 8**.

Box-Pierce Q Statistical Test

Box-Pierce Q Statistical test was carried out to determining whether there is white noise in the residual of the observed and predicted tidal data. The auto correlations at lags 1 to 30 were computed using Eq. 13 given by Box, Jenkins, Reinsel and Ljung (2015).

$$r_k = \frac{\sum_{t=k+1}^{n}([y_t - \bar{y}][y_{t-k} - \bar{y}])}{\sum_{t=1}^{n}(y_t - \bar{y})^2} \qquad (13)$$

where, r_1 shows how successive values of y relate to each other, r_2 shows how y values two periods apart relate to each other, and, r_n shows how y values n periods apart relate to each other. The auto correlations at lag 1, 2, …, make up the autocorrelation function (ACF).

Table 8: Sample Observed and Predicted Tidal Data above Chart Datum

S/N	Year	Month	Day	Hour	Observed Tide (m)	Predicted Tide (m)	Difference (m)
1	2010	9	11	18	1.6660	1.6655	0.0005
2	2010	9	11	19	1.5630	1.5633	-0.0003
3	2010	9	11	20	1.2980	1.2978	0.0002
4	2010	9	11	21	0.9330	0.9329	0.0001
5	2010	9	11	22	0.5720	0.5723	-0.0003
6	2010	9	11	23	0.3260	0.3256	0.0004
7	2010	9	12	0	0.2650	0.2651	-0.0001
8	2010	9	12	1	0.4010	0.4008	0.0002
9	2010	9	12	2	0.6850	0.6849	0.0001
10	2010	9	12	3	1.0380	1.0384	-0.0004
11	2010	9	12	4	1.3800	1.3799	0.0001
12	2010	9	12	5	1.6400	1.6404	-0.0004
13	2010	9	12	6	1.7660	1.7661	-0.0001
14	2010	9	12	7	1.7220	1.7218	0.0002
15	2010	9	12	8	1.5050	1.5045	0.0005
16	2010	9	12	9	1.1570	1.1574	-0.0004
17	2010	9	12	10	0.7690	0.7691	-0.0001
18	2010	9	12	11	0.4470	0.4474	-0.0004
19	2010	9	12	12	0.2790	0.2795	-0.0005
20	2010	9	12	13	0.2990	0.2987	0.0003
21	2010	9	12	14	0.4800	0.4800	0.0000
22	2010	9	12	15	0.7600	0.7599	0.0001
23	2010	9	12	16	1.0650	1.0647	0.0003
24	2010	9	12	17	1.3290	1.3294	-0.0004
25	2010	9	12	18	1.5010	1.5008	0.0002
26	2010	9	12	19	1.5390	1.5386	0.0004
27	2010	9	12	20	1.4250	1.4252	-0.0002
28	2010	9	12	21	1.1810	1.1808	0.0002
29	2010	9	12	22	0.8700	0.8703	-0.0003
30	2010	9	12	23	0.5880	0.5881	-0.0001

A white noise model is a model where observations y_t is made of two parts: a fixed value C and an uncorrelated random error component e_r as in Eq. 14.

$$y_t = C + e_r \tag{14}$$

For uncorrelated data (a time series which is white noise) we expect each autocorrelation to be close to zero.

The error component in this work was determined by using the relation expressed in Eq. 15:

$$e_r = yobs_t - ypre_t \tag{15}$$

where, $yobs_t$ is observed tidal data at time t and $ypre_t$ is the predicted tidal data at time t.

The autocorrelations at lags 1 to 30 were computed using equation 3.1. The results of the auto correlations at lags 1 to 30 are given in **Table 9**. **Figure 1** and **Figure 2** show autocorrelations at lags 1 to 30 and the residuals of the observed and predicted tides respectively.

Table 9: Autocorrelation at Lags 1 to 30

S/N	R_X	Value of R_X
1	R_1	-0.0293
2	R_2	0.0289
3	R_3	0.0157
4	R_4	-0.0137
5	R_5	-0.0195
6	R_6	0.0339
7	R_7	-0.0336
8	R_8	0.0071
9	R_9	-0.0315
10	R_{10}	-0.0071
11	R_{11}	0.0077
12	R_{12}	-0.0059
13	R_{13}	-0.0085
14	R_{14}	-0.0316
15	R_{15}	-0.0336
16	R_{16}	0.0078
17	R_{17}	-0.0051
18	R_{18}	0.0118
19	R_{19}	0.0055
20	R_{20}	0.0016
21	R_{21}	0.0235
22	R_{22}	-0.0091
23	R_{23}	-0.0420
24	R_{24}	-0.0358
25	R_{25}	0.0241
26	R_{26}	-0.0131
27	R_{27}	0.0070
28	R_{28}	-0.0351
29	R_{29}	-0.0035
30	R_{30}	-0.0186

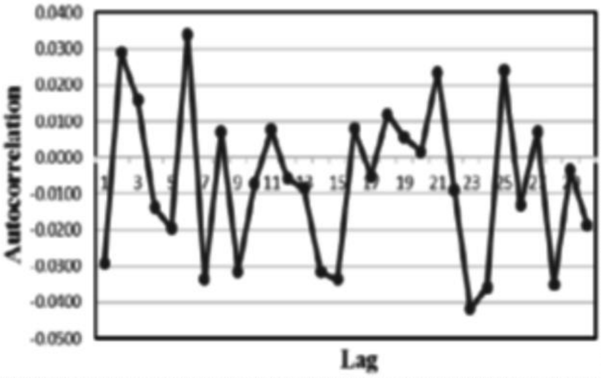

Figure 1: Autocorrelations at lag 1 to 30

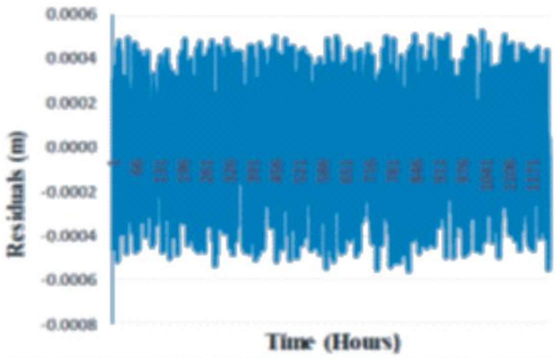

Figure 2: Residuals of Observed and Predicted Tides

For 95% confidence interval, it is expected that about 95% of the autocorrelations for the 30 lags should be within $-1.96\sqrt{\frac{1}{n}} \leq r_k \leq 1.96\sqrt{\frac{1}{n}}$; therefore $-0.056 \leq r_k \leq 0.056$. The autocorrelation for all the 30 lags falls within the range. There is no significant correlation in the range of the 30 lags. We, therefore, conclude that the series of residuals of the observed and predicted data is white noise.

Root Mean Square Error

The Root-Mean-Square error (RMSE) of the observed and predicted hourly tides was found using Eq. 16.

$$RMSE = \sqrt{\left(\frac{1}{n}\sum_{i=1}^{n} e_i^2\right)} \quad (16)$$

where, e_i = predicted tide at time i is the observed tide at time I, n = 1224 and RMSE = 0.0003m

4.0 CONCLUSION

In this work, 1224 hourly water level tidal data derived from pressure data recorded by WLR 7 water level recorder at water depth of 1,000 m at Bonga oilfield were used to do least squares tidal harmonic analysis.

From the least squares tidal harmonic analysis, the amplitudes and the phase lags for eleven tidal constituents were computed and tidal predictions starting from the initial time of observation in September 11, 2010 to January 2019 were made at 10 minutes' intervals.

Statistical analysis of the predicted tides with validation data was made and the maximum deviation of the predicted tides from the observed data is 0.0008 m, while the Root Mean Square Error is 0.0003 m. Autocorrelation at lags 1 to 30 for the residuals of the observed and predicted tidal data shows that there is no significant correlation in the range of the 30 lags. We, therefore, conclude that the series of residuals of the observed and predicted data is white noise. The accuracy achieved in this work is high enough for offshore marine operations in Bonga Field.

4.1 Recommendations

The following recommendations are made based on the results of this work:

- Tidal data derived from water level recorders covering a period of at least one year should be collected at deep offshore and near shore water locations to improve the accuracy of tidal harmonic analysis and prediction.
- The accuracy of this work is high enough to support deep and shallow water operations in oil and gas industries.
- Water level recorders or buoys capable of being tracked by satellites should be placed at various locations within the Nigerian coastal waters for further tidal studies.

REFERENCES

Badejo, O.T., Evarie, P., Alademoni, S and Anorue, N., (2013). Tidal Harmonic Analysis at Bonga Field. *Fédération Internationale des Géomètres (FIG) 2013 Regional Conference*. Abuja, Nigeria.

Box, G.E.P. and Jenkins, G.M. (1972). Time series analysis, forecasting and control, Holden Day Inc., San Francisco, United States of America.

Doodson, A. T. and Warburg, H. D., (1941). Admiralty Manual of Tides, Hydrographic Department, Admiralty. United Kingdom. 270pp.

Eluwa, E.C., (1991). Prediction of Vertical Tides by Least Squares Harmonic Analysis. M.Sc. Degree Project. Department of Surveying and Geoinformatics, University of Lagos, (Unpublished).

Schureman, P., (1958). Manual of harmonic analysis and prediction of tides. Department of Commerce, Coast and Geodetic Survey, Special Publication No. 98. U.S. Government Printing Office, Washington. United States of America. 317pp

Stravisi, F., (1983). The IT Method for the Harmonic Tidal Prediction. *Bollrtino Di Oceanologia Ed Applicata*, 1**(3):** 193-204.